JACS
JOURNAL OF THE AMERICAN CHEMICAL SOCIETY
Communication
pubs.acs.org/JACS

Crystal Structure of the Glycophorin A Transmembrane Dimer in Lipidic Cubic Phase

Raphael Trenker,[†,‡] Matthew E. Call,*[,†,‡] and Melissa J. Call*[,†,‡]

[†]Structural Biology Division, The Walter and Eliza Hall Institute of Medical Research, Parkville, Victoria 3052, Australia
[‡]Department of Medical Biology, The University of Melbourne, Parkville, Victoria 3052, Australia

Supporting Information

ABSTRACT: The mechanisms of assembly and function for many important type I/II (single-pass) transmembrane (TM) receptors are proposed to involve the formation and/or alteration of specific interfaces among their membrane-embedded α-helical TM domains. The application of lipidic cubic phase (LCP) bilayer media for crystallization of single-α-helical TM complexes has the potential to provide valuable structural and mechanistic insights into many such systems. However, the fidelity of the interfaces observed in crowded crystalline arrays has been difficult to establish from the very limited number of such structures determined using X-ray diffraction data. Here we examine this issue using the glycophorin A (GpA) model system, whose homodimeric TM helix interface has been characterized by solution and solid-state NMR and biochemical techniques but never crystallographically. We report that a GpA-TM peptide readily crystallized in a monoolein cubic phase bilayer, yielding a dimeric α-helical structure that is in excellent agreement with previously reported NMR measurements made in several different types of host media. These results provide compelling support for the wider application of LCP techniques to enable X-ray crystallographic analysis of single-pass TM interactions.

The transmembrane (TM) regions of single-spanning membrane proteins guide intermolecular interactions that regulate their functions and oligomeric distributions. Examples include a number of important therapeutic targets such as receptor-tyrosine kinases,[1] cytokine and growth hormone receptors,[2−4] cell adhesion proteins,[5] and activating immune receptors.[6] Characterizing the structural features governing these interactions can thus provide unique insights into the biologically active forms of receptor complexes and the mechanisms they employ to communicate information across the cell membrane. The small number of available structures of single-TM complexes have been determined primarily using solution NMR methods applied to detergent micelle or small isotropic bicelle-embedded systems.[7] The major barriers to broader application of these techniques arise from limits on peptide solubility in NMR-compatible lipids and detergents, the high propensity of hydrophobic TM peptides to aggregate nonspecifically, and the challenges involved in identifying a sufficient number of unambiguous long-range distance restraints from which to calculate structures. Alternative approaches for gaining high-resolution structural information on TM peptide targets are therefore highly desirable. The use of lipidic cubic phases (LCP) as host media for "*in meso*" crystallization has recently emerged as a major enabling technology in membrane protein structural analysis.[8,9] However, the application of LCP techniques to small membrane-associated peptides has been extremely limited,[10−13] and only two published examples involve α-helical TM sequences derived from naturally occurring single-pass membrane proteins.[12,13] As such, significant questions remain regarding the general suitability of the technique for determining the biologically relevant structures of single-TM interfaces. In this study, we wished to examine whether physiological packing modes are maintained in the context of a crowded crystalline array and what impact the nature of the host medium has on the configuration of single-TM interfaces. To address these issues, we determined the crystal structure of the glycophorin A (GpA) TM domain, whose dimeric interface has been thoroughly characterized using several different biochemical[14−16] and spectroscopic[17−20] methods, but never crystallographically.

We first examined whether a recombinantly produced GpA TM peptide (GpA-TM, Figure 1a) could be effectively reconstituted into the cubic phase in a state that allows free lateral diffusion to support crystal growth. Reconstitution is commonly achieved using a solution of detergent-solubilized protein that is mixed with an LCP-forming host lipid.[9] However, for small helical peptides that refold easily it is also possible to precombine peptide and lipid in organic solvent, remove the solvent by evaporation, and form the cubic phase by mixing with pure water or buffer solution.[10,12] A fraction of purified GpA-TM was fluorescently labeled with cyanine3 maleimide at an engineered C-terminal cysteine to measure fluorescence recovery after photobleaching (FRAP). LCP-FRAP has been successfully used to determine diffusion kinetics and mobile protein fraction for GPCRs, and both parameters positively correlate with crystallization.[21,22] High diffusible fractions (above 70%) were obtained for peptides reconstituted from hexafluoroisopropanol (HFIP) and from the detergents *n*-dodecyl β-D-maltoside (DDM), tetradecylphosphocholine (TDPC), and lysomyristoylphosphatidylglycerol (LMPG) (Supplementary Figure 1). The fastest diffusion rate and the highest fluorescence recovery during the 5 min analysis time were observed in the detergent-free HFIP sample. Since this

Received: November 5, 2015
Published: December 8, 2015

DOI: 10.1021/jacs.5b11354
J. Am. Chem. Soc. 2015, 137, 15676−15679

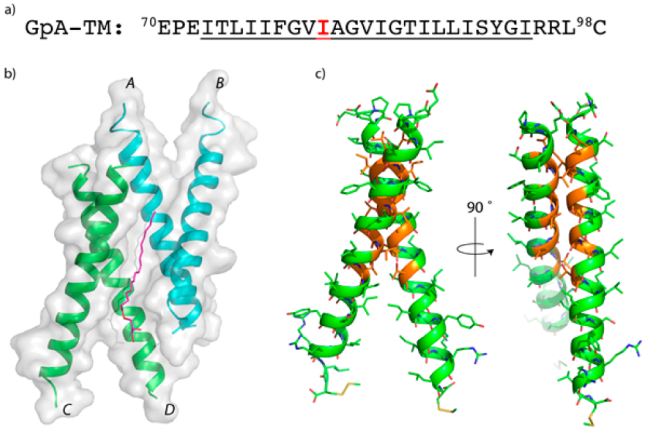

Figure 1. Structure of a Glycophorin A TM peptide crytallized in a monoolein lipidic cubic phase. (a) A GpA TM peptide with residues E70 to L98 including a C-terminal Cys was used for crystallization. The M81I substitution was introduced for production purposes (see methods) and is shown in red, the helical TM region is underlined. (b) Two GpA-TM dimers and a structured monoolein form the asymmetric unit of the crystal. (c) The GpA-TM structure with the dimerization interface LIxxGVxxGVxxT shown in orange. PDB code 5EH4.

procedure eliminated detergent choice as a variable and supported high peptide concentrations in the lipid phase, we opted to screen for crystallization conditions by reconstituting GpA-TM peptide into monoolein from HFIP to a final concentration of 40 mg/mL in the LCP sample. The engineered C-terminal cysteine was retained in the peptide used for crystallization screening, but the side-chain thiol was protected by reaction with S-methylmethanethiosulfonate. At least two different crystal forms were identifiable at time points from 2 to 48 h after setup and in 26 out of 384 conditions tested. Data sets recorded from two isomorphous crystals grown in an optimization screen around one of these conditions (0.1 M HEPES pH 7.5, 20% (w/v) PEG 8000) were merged to solve the structure of the GpA TM domain to 2.81 Å resolution. The asymmetric unit contains two parallel GpA-TM dimers (Figure 1b; deposited in the PDB as 5EH4) packed in an antiparallel orientation to each other through extensive contacts along helices A and D, with a single structured monoolein in the center. Dimer AB (cyan) and dimer CD (green) align with a backbone RMSD of 0.3 Å in the TM region (I73-I95). Each of the two dimers has a right-handed crossing angle of −37° and features a close packing interface via the LIxxGVxxGVxxT motif (Figure 1c, orange) that was first identified by mutagenesis[14,15] and later observed in the solution NMR structure.[17] As in other LCP structures, the lattice shows type-1 packing (Figure 2) with the long axis of the unit cell perpendicular to the plane of the lipid bilayer. N- and C-termini of the GpA-TM peptides contact adjacent layers to extend the lattice, and additional lateral contacts revealed no alternative parallel interfaces. A second crystal form, often coexisting in the same drop with the dimer crystals, contained only one GpA-TM helix per asymmetric unit that formed no parallel interfaces with neighboring peptides in the crystal lattice (deposited in the PDB as 5EH6). This suggests that a monomer−dimer equilibrium existed in the lipid phase and that the two species segregated during crystallization.

This structure provides a unique opportunity to compare the packing of a simple TM helix dimer crystallized from a lipid

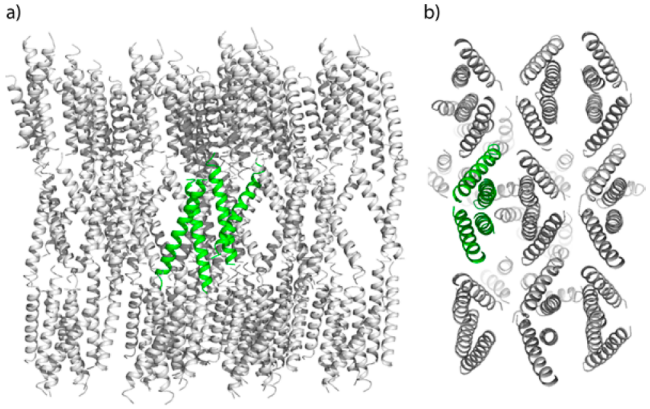

Figure 2. Molecular organization within the GpA-TM LCP crystals. Dimers are arranged within the LCP bilayer in alternating orientations with two dimers per asymmetric unit (green). N- and C-terminal residues of the individual GpA-TM helices contact adjacent layers. Views are shown parallel (a) and perpendicular (b) to the lamellar plane.

bilayer environment with existing NMR structures of the same interface determined in several different types of host media. Structures of the GpA TM interface have been calculated from $^{1}H-^{1}H$ NOE restraints measured by solution NMR in DPC micelles[17,18] and DMPC/DHPC bicelles,[18] as well as from ^{13}C dipolar coupling restraints measured by solid-state magic angle spinning (MAS) NMR in phospholipid bilayers.[19,20,23] The crystal structure aligns well with representative structures from each solution NMR ensemble and the ssNMR model (Figure 3a), yielding pairwise RMSD values well below 1 Å in the core helical region (I73-I95) and less than 0.6 Å in the region of the dimerization interface (L75-T87) only. Mirroring the divergence in the solution NMR ensembles near the helix ends, the B-factors in the LCP crystal structure are lowest in the native

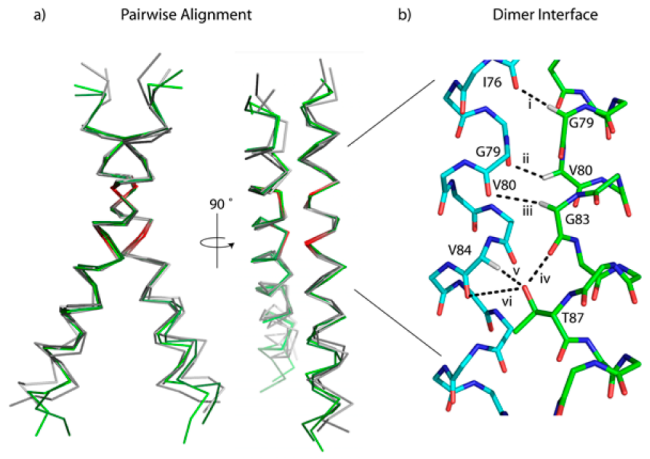

Figure 3. Alignment of GpA-TM structures and interface hydrogen bond network. (a) Pairwise backbone alignments of the dimerization interface region (L75-T87) of the 5EH4 AB dimer (dark green), 1AFO (micelle) state 19 (light gray), 2KPF (bicelle) state 4 (dark gray), and ssNMR structures onto the 5EH4 CD dimer (light green) are shown and are all below 0.6 Å. G79 and G83 are colored in red for reference. (b) The proposed backbone−backbone hydrogen bond network at the dimer interface is formed between I76-G79 (i), G79−80 (ii), and V80-G83 (iii). The T87 hydroxyl group has been proposed to form an intramolecular hydrogen bond to G83 (iv) and two possible intermolecular hydrogen bonds to V84 (v, vi).

DOI: 10.1021/jacs.5b11354
J. Am. Chem. Soc. 2015, 137, 15676−15679

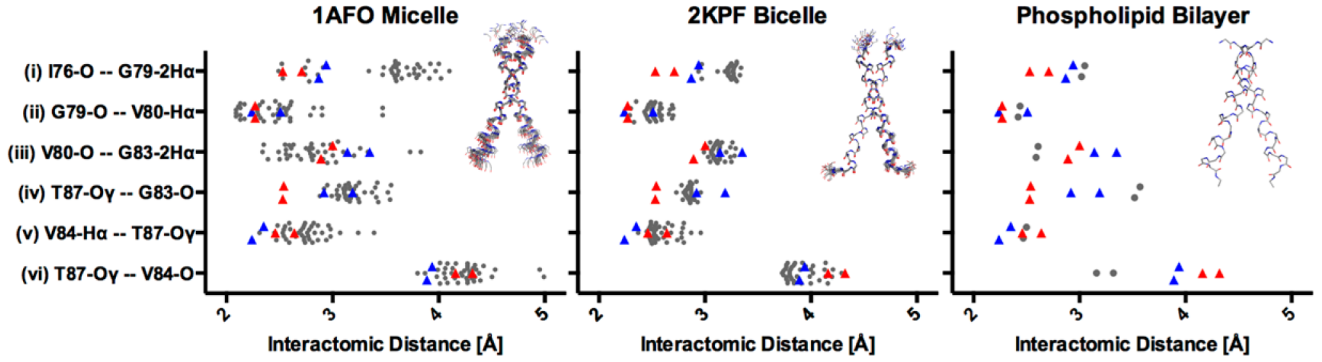

Figure 4. Comparison of interatomic distance measurements for key interface contacts in LCP and NMR structures. For each contact identified in Figure 3b, 40 interatomic distances are plotted as gray dots for each solution NMR structure ensemble (two symmetrical contacts for the 20 structures in 1AFO and 2KPF ensembles) and two for the single solid-state NMR structure (structures shown in upper right corners). Two measurements from each of the two dimers in the 5HE4 asymmetric unit (red triangles, dimer CD; blue triangles, dimer AB) are superimposed on each plot of NMR distances for comparison.

interface and increase with distance from the core packing region (see Supplementary Figure 2 for omit density maps and B-factor analysis).

The defining feature of the GpA dimer interface is the close helix−helix packing around the $G^{79}xxxG^{83}$ motif that provides favorable van der Waals contacts and facilitates backbone−backbone interactions via noncanonical CαH−O hydrogen bonds.[24] Three such interactions have been identified at I76-G79, G79-V80, and V80-G83 (Figure 3b, contacts *i, ii, iii*).[24] While H atoms are not directly observable in our electron density at this resolution, they can be placed in the model with high confidence to examine these interactions. A comparison of the relevant interatomic distances among the NMR and crystal structures (Figure 4) shows that the 5EH4 (LCP) measurements fall generally within the range of distances observed in the 1AFO (micelle) and 2KPF (bicelle) ensembles, as do the solid state NMR measurements, though for I76-G79 (contact *i*) the LCP distances cluster with a minor population of the closest packed solution NMR structures. Based on mutagenesis experiments[14,15] and free energy measurements,[25] the T87 side-chain hydroxyl is also thought to participate in stabilizing interhelical hydrogen bonds. The solution NMR structures suggest that this group acts simultaneously as a donor in an intrahelical hydrogen bond to the *i*-4 (G83) backbone carbonyl oxygen (Figure 3b, contact *iv*) and an acceptor to the V84 CαH on the opposing monomer (contact *v*). Based on solid-state NMR measurements, Smith et al.[23] proposed that the T87 hydroxyl acts instead as a donor for an interhelical hydrogen bond to the V84 backbone carbonyl oxygen (Figure 3b, contact *vi*). Our measurements in this region (Figure 4) are in good agreement with the solution NMR data and do not support this alternative hydrogen bond, though we note that the differences are generally small (1 Å or less) and our data do not rule out the possibility that this conformation is unique to the phospholipid conditions used to make the solid-state NMR measurements.

The general concordance of the GpA-TM crystal structure with mutagenesis data and previously determined NMR structures provides compelling evidence that crystallization in an appropriate lipid bilayer medium can reveal the physiologically relevant packing interfaces even for small, very hydrophobic peptides. The recently published structures of the tetrameric influenza M2 proton channel at 1.10 Å resolution in LCP further highlight the utility of the technique for a similar class of "minimalist" membrane proteins. Our analysis demonstrates that, in the case of GpA, the dimeric association is dominated by protein−protein interactions to the extent that structures determined in four very different types of membrane or membrane-like host media show only very minor differences. Furthermore, the presence of extended non-native (antiparallel) contacts between neighboring dimers does not appear to have perturbed the native interface in the LCP crystal lattice. It is notable that the GpA-TM peptide readily crystallized despite the inclusion of membrane-proximal sequences that were very poorly ordered in the solution NMR structures (N-terminal EPE; C-terminal RRL), and this example provides a template for the design of appropriate peptide constructs for crystallographic studies of other single-pass TM interactions. We anticipate that these methods will prove applicable to a broad array of important receptor systems and provide a powerful complementary and/or alternative approach to the spectroscopic methods that are currently the standard for structural analysis of this challenging class of membrane protein targets.

■ ASSOCIATED CONTENT

Supporting Information

The Supporting Information is available free of charge on the ACS Publications website at DOI: 10.1021/jacs.5b11354.

Experimental methods, supplementary figures, and tables (PDF)

■ AUTHOR INFORMATION

Corresponding Authors

*call@wehi.edu.au (M.E.C.)
*call@wehi.edu.au (M.J.C.)

Notes

The authors declare no competing financial interest.

■ ACKNOWLEDGMENTS

We thank Kelly Rogers and Mark Scott at the WEHI Imaging Facility for assistance with FRAP analysis, Janet Newman for materials, Jacqui Gulbis for helpful advice on structure refinement, Steven O. Smith for provision of the ssNMR structure coordinates, and Cyrus Tan and Logesvaran Krshnan for helpful discussions. We acknowledge the use of the CSIRO Collaborative Crystallization Centre (C3) for LCP screening. Part of this research was carried out at the MX2 beamline of the

DOI: 10.1021/jacs.5b11354
J. Am. Chem. Soc. 2015, 137, 15676−15679

Australian Synchrotron, and we thank the beamline scientists for their technical support. This work was supported by the Human Frontier Science Program (Grant RGP0064 to M.E.C.) and the National Health and Medical Research Council (Project Grant 1030902 to M.E.C. and M.J.C.; IRIISS Infrastructure Support to WEHI). M.E.C. is supported by ARC QEII Fellowship DP110104369. M.J.C. is supported by ARC Future Fellowship FT120100145.

REFERENCES

(1) Endres, N. F.; Das, R.; Smith, A. W.; Arkhipov, A.; Kovacs, E.; Huang, Y.; Pelton, J. G.; Shan, Y.; Shaw, D. E.; Wemmer, D. E.; Groves, J. T.; Kuriyan, J. *Cell* **2013**, *152*, 543.
(2) Brooks, A. J.; Dai, W.; O'Mara, M. L.; Abankwa, D.; Chhabra, Y.; Pelekanos, R. A.; Gardon, O.; Tunny, K. A.; Blucher, K. M.; Morton, C. J.; Parker, M. W.; Sierecki, E.; Gambin, Y.; Gomez, G. A.; Alexandrov, K.; Wilson, I. A.; Doxastakis, M.; Mark, A. E.; Waters, M. J. *Science* **2014**, *344*, 1249783.
(3) Constantinescu, S. N.; Keren, T.; Socolovsky, M.; Nam, H.; Henis, Y. I.; Lodish, H. F. *Proc. Natl. Acad. Sci. U. S. A.* **2001**, *98*, 4379.
(4) Livnah, O.; Stura, E. A.; Middleton, S. A.; Johnson, D. L.; Jolliffe, L. K.; Wilson, I. A. *Science* **1999**, *283*, 987.
(5) Kim, M.; Carman, C. V.; Springer, T. A. *Science* **2003**, *301*, 1720.
(6) Call, M. E.; Wucherpfennig, K. W. *Nat. Rev. Immunol.* **2007**, *7*, 841.
(7) Call, M. E.; Chou, J. J. *Structure* **2010**, *18*, 1559.
(8) Landau, E. M.; Rosenbusch, J. P. *Proc. Natl. Acad. Sci. U. S. A.* **1996**, *93*, 14532.
(9) Caffrey, M.; Cherezov, V. *Nat. Protoc.* **2009**, *4*, 706.
(10) Hofer, N.; Aragao, D.; Caffrey, M. *Biophys. J.* **2010**, *99*, L23.
(11) Joh, N. H.; Wang, T.; Bhate, M. P.; Acharya, R.; Wu, Y.; Grabe, M.; Hong, M.; Grigoryan, G.; DeGrado, W. F. *Science* **2014**, *346*, 1520.
(12) Knoblich, K.; Park, S.; Lutfi, M.; van 't Hag, L.; Conn, C. E.; Seabrook, S. A.; Newman, J.; Czabotar, P. E.; Im, W.; Call, M. E.; Call, M. J. *Cell Rep.* **2015**, *11*, 1184.
(13) Thomaston, J. L.; Alfonso-Prieto, M.; Woldeyes, R. A.; Fraser, J. S.; Klein, M. L.; Fiorin, G.; DeGrado, W. F. *Proc. Natl. Acad. Sci. U. S. A.* **2015**, *112*, 14260.
(14) Lemmon, M. A.; Flanagan, J. M.; Hunt, J. F.; Adair, B. D.; Bormann, B. J.; Dempsey, C. E.; Engelman, D. M. *J. Biol. Chem.* **1992**, *267*, 7683.
(15) Lemmon, M. A.; Flanagan, J. M.; Treutlein, H. R.; Zhang, J.; Engelman, D. M. *Biochemistry* **1992**, *31*, 12719.
(16) Zhu, J.; Luo, B. H.; Barth, P.; Schonbrun, J.; Baker, D.; Springer, T. A. *Mol. Cell* **2009**, *34*, 234.
(17) MacKenzie, K. R.; Prestegard, J. H.; Engelman, D. M. *Science* **1997**, *276*, 131.
(18) Mineev, K. S.; Bocharov, E. V.; Volynsky, P. E.; Goncharuk, M. V.; Tkach, E. N.; Ermolyuk, Y. S.; Schulga, A. A.; Chupin, V. V.; Maslennikov, I. V.; Efremov, R. G.; Arseniev, A. S. *Acta Naturae* **2011**, *3*, 90.
(19) Smith, S. O.; Jonas, R.; Braiman, M.; Bormann, B. J. *Biochemistry* **1994**, *33*, 6334.
(20) Smith, S. O.; Song, D.; Shekar, S.; Groesbeek, M.; Ziliox, M.; Aimoto, S. *Biochemistry* **2001**, *40*, 6553.
(21) Cherezov, V.; Liu, J.; Griffith, M.; Hanson, M. A.; Stevens, R. C. *Cryst. Growth Des.* **2008**, *8*, 4307.
(22) Fenalti, G.; Abola, E. E.; Wang, C.; Wu, B.; Cherezov, V. *Methods Enzymol.* **2015**, *557*, 417.
(23) Smith, S. O.; Eilers, M.; Song, D.; Crocker, E.; Ying, W.; Groesbeek, M.; Metz, G.; Ziliox, M.; Aimoto, S. *Biophys. J.* **2002**, *82*, 2476.
(24) Senes, A.; Ubarretxena-Belandia, I.; Engelman, D. M. *Proc. Natl. Acad. Sci. U. S. A.* **2001**, *98*, 9056.
(25) Hong, H.; Blois, T. M.; Cao, Z.; Bowie, J. U. *Proc. Natl. Acad. Sci. U. S. A.* **2010**, *107*, 19802.

DOI: 10.1021/jacs.5b11354
J. Am. Chem. Soc. 2015, 137, 15676−15679